










NUMERICAL SIMULATIONS OF RECENT AND FUTURE EVOLUTION OF MONTE PERDIDO GLACIER

ANNA MATEOS-GARCIA^{1,2*} , MARÍA SANTOLARIA-OTÍN² ,
YOLANDA SOLA² , ESTEBAN ALONSO-GONZÁLEZ^{3,1} ,
JAIME OTERO⁴ , LUIS MARIANO DEL RIO⁵,
JUAN IGNACIO LÓPEZ-MORENO¹ , JESÚS REVUELTO¹ 

¹*Instituto Pirenaico de Ecología (CSIC), Avda Montañana 1005, 50080 Zaragoza, Spain.*

²*Grup de Meteorologia, Departament de Física Aplicada, Facultat de Física, Universitat de Barcelona, Martí i Franquès, 08028 Barcelona, Spain.*

³*Centre d'Etudes Spatiales de la Biosphère, Université de Toulouse, CNRS–CNES–IRD–INRA–UPS, Toulouse, France.*

⁴*Departamento de Matemática Aplicada a las Tecnologías de la Información y las Comunicaciones, E.T.S.I. de Telecomunicación, Universidad Politécnica de Madrid, Av. Complutense, 30, ES-28040 Madrid, Spain.*

⁵*Departamento de Física Aplicada. Escuela Politécnica, Universidad de Extremadura, Cáceres 10071, Spain.*

ABSTRACT. Glaciers are globally retreating due to climate change, and the Pyrenees Mountain range is no exception. This study uses the Open Global Glacier Model (OGGM) to explore the dynamics of the Monte Perdido glacier, one of the largest remaining glaciers in the Pyrenees. We explored three calibration approaches to assess their performances when reproducing observed volume decreases. The first approach involved mass balance calibration using terrestrial laser scanning data from 2011 to 2022 and climate data from a nearby weather station. The second approach used terrestrial laser scanning calibration with default climate data provided by OGGM (GSWP3-W5E5). The third approach used default geodetic mass balance calibration and default climate data. By comparing these calibration strategies and analysing historical data (terrestrial laser scanning and ground penetrating radar), we obtain insights of the applicability of OGGM to this small, mild conditions, Pyrenean glacier. The first calibration approach is identified as the most effective, emphasising the importance of selecting appropriate climate data and calibration methods. Additionally, we conducted future volume projections using an ensemble of General Circulation Models (GCMs) under the RCP2.6 and RCP8.5 scenarios. The results indicate a potential decrease in total ice volume ranging from 91.60% to 95.16% by 2100, depending on the scenario. Overall, this study contributes to the understanding of the Monte Perdido glacier's behaviour and its response to climate change through the calibration of the OGGM, while also providing the first estimate of its future melting under different emission scenarios.

Simulaciones numéricas de la evolución reciente y futura del glaciar Monte Perdido

RESUMEN. Los glaciares están retrocediendo globalmente debido al cambio climático, y la cordillera de los Pirineos no es una excepción. Este estudio utiliza el modelo Open Global Glacier (OGGM) para explorar la dinámica del glaciar Monte Perdido, uno de los glaciares actuales de mayor tamaño de los Pirineos. Se exploran tres enfoques de calibración para evaluar sus rendimientos al reproducir las disminuciones de volumen observadas. El primer enfoque

consistió en calibrar el balance de masas utilizando datos de escaneo láser terrestre de 2011 a 2022 y datos climáticos de una estación meteorológica cercana. El segundo enfoque utilizó la calibración de escaneo láser terrestre con datos climáticos predeterminados proporcionados por OGGM (GSWP3-W5E5). El tercer enfoque manejó la calibración geodésica predeterminada del balance de masas y los datos climáticos predeterminados. Al comparar estas estrategias de calibración y analizar los datos históricos (escaneo láser terrestre y radar de penetración en el suelo), se obtiene información sobre la aplicabilidad del OGGM a este pequeño glaciar pirenaico. Se considera que el primer método de calibración es el más eficaz, haciendo hincapié en la importancia de seleccionar los datos climáticos y los métodos de calibración adecuados. Además, se realizaron proyecciones de volumen futuras utilizando un conjunto de modelos de circulación general (GCMs) bajo los escenarios RCP2.6 y RCP8.5. Los resultados indican una disminución potencial en el volumen total de hielo que va del 91,60% al 95,16% para 2100, dependiendo del escenario. En general, este estudio contribuye a la comprensión del comportamiento del glaciar Monte Perdido y su respuesta al cambio climático a través de la calibración del OGGM, al tiempo que proporciona la primera estimación de su futura fusión bajo diferentes escenarios de emisión.

Keywords: Mountain glacier, OGGM, in-situ surface observations, climate change.

Palabras clave: Glaciar de montaña, OGGM, observaciones superficiales in-situ, cambio climático.

Received: 11 August 2023

Accepted: 24 November 2023

***Corresponding author:** Anna Mateos García and Jesús Revuelto, Instituto Pirenaico de Ecología (CSIC), Avda. Montañana 1005, 50080 Zaragoza, Spain. E-mail: annamateosg@gmail.com; jrevuelto@ipe.csic.es

1. Introduction

Glaciers are highly sensitive indicators of recent climate variations (Beniston, 2003; Grunewald and Scheithauer, 2010). Current assessments of the Intergovernmental Panel on Climate Change (IPCC) have highlighted that changes in temperature and precipitation have resulted in global glacier retreat since the 1950s that is unprecedented in the last 2000 years (IPCC, 2021).

Glaciers in the Pyrenees are currently in a critical situation, with clear evidence of very advanced stages of degradation (Rico *et al.*, 2017; Vidaller *et al.*, 2021). Due to their small dimensions, glaciers in the Pyrenees have minimal impact on water resources and global albedo feedback (López-Moreno *et al.*, 2020). However, they hold scientific and touristic value while carrying strong cultural heritage (García-López *et al.*, 2021; Moreno *et al.*, 2021; Serrano Cañadas, 2023). Therefore, their melting represents a significant event, symbolising the wider consequences of climate change.

Glaciers, characterized by compact, perennial ice, experience mass gain through snow accumulation and mass loss during ablation, primarily through surface melting (van der Veen, 2013; Eis, 2020). The balance between accumulation and ablation determines a glacier mass fluctuations, with retreat occurring when ablation surpasses accumulation.

Glacier dynamics of mass balance respond to climate fluctuations on longer time scales rather than immediately (Huston *et al.*, 2021). Consequently, the advance or retreat of a glacier is not only determined by the weather of a single year but is a response to cumulative forcings from many years (Huybers and Roe, 2009). Furthermore, there are other processes that influence glacier evolution such as avalanches, being sheltered from dominant winds, debris cover thickness, slope of the ice surface, or rocky outcrops that may appear and enhance incoming long-wave radiation (López-Moreno *et al.*, 2019).

Given the urgency of climate change and glacier retreat, there is significant motivation to study glacier dynamics through a modelling approach, allowing for predictions of future volume trends given climatic and geographic inputs. Hence, this study aims to explore the performance of a glacier model and its practical implementation for the Monte Perdido glacier, one of the largest remaining glaciers in the Pyrenees (Vidaller *et al.*, 2021), with noticeable thinning observed in recent years (López-Moreno *et al.*, 2019).

2. Study area

The Monte Perdido glacier, located in the Ordesa and Monte Perdido National Park in the Central Spanish Pyrenees (42.6806°N, 0.0375°E), consisted of two ice bodies until 2021: the upper and lower glaciers (Fig. 1). Both bodies are north facing and lie beneath the Monte Perdido Peak (3355 m a.s.l.). The mean elevations of the upper and lower ice bodies are between 3110 and 2885 m a.s.l., respectively (Julián and Chueca, 2007). In 2022, the lower Monte Perdido glacier experienced a division, resulting in the formation of two separate ice bodies (Fig. 1).

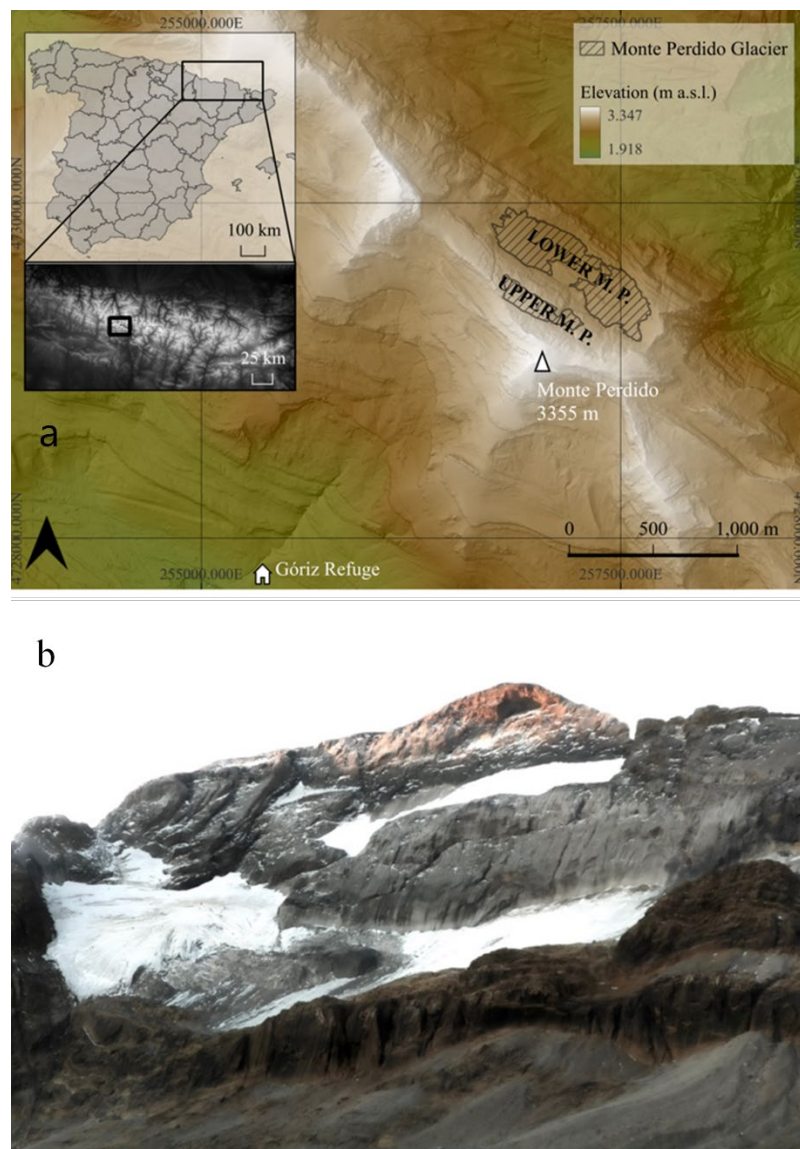


Figure 1: (a) Location and extent of the Monte Perdido glacier in 2022 (coordinates in extended UTM zone 31 T). (b) View of Monte Perdido glacier on October 5, 2022.

3. Data and methodology

3.1. Data analysis tools

To simulate and analyse the Monte Perdido glacier, we utilised the Open Global Glacier Model (OGGM), which is a Python based open-source model (Maussion *et al.*, 2019). We employed version 1.6.0 of OGGM, which was released on March 10, 2023 (Maussion *et al.*, 2023). With the glacier outlines, topographical data, and climate data at a reasonable resolution, the model can estimate the total ice volume of the glacier and simulate its dynamic evolution in response to different climate forcings (Maussion *et al.*, 2019). To compute the ice thickness, the model uses an ice thickness inversion method based on Farinotti *et al.*, (2009).

OGGM is a flowline model that simplifies the glacier geometry by representing it as lines that depict the central flow path. The flowlines are defined following the approach described by Kienholz *et al.*, 2014. The model employs the isothermal shallow ice approximation, assuming that the ice thickness is small compared to its lateral extent, meaning that x-derivatives of stress and velocity are small compared with the z-derivatives (Paterson, 2000). It is important to note that the shallow ice approximation is primarily intended for large ice shelves and may not fully capture the complexities of small mountain glaciers like Monte Perdido. For this glacier, it would be more appropriate to use a model that solves the complete Stokes system, accounting for the three-dimensional nature of ice flow. However, for the sake of simplicity and computational efficiency, we opted to use the OGGM model for this study. Despite this limitation, the validation process supports its use for our specific objectives.

In addition, we used QGIS and CloudCompare software, both open-source platforms, to acquire the outlines of the glacier derived from TLS and compare glacier surface differences between the TLS and OGGM model.

3.2. Glacier observation dataset

The surface of the Monte Perdido glacier was derived from terrestrial laser scanning (TLS, RIEGL LPM-321), following the methodology described by López-Moreno *et al.*, (2016). This device generates a 3D point cloud by measuring the distance to thousands of points of the target area with LiDAR technology (Revuelto *et al.*, 2014). TLS observations from 2011 to 2022, allowed us to diagnose the current state of the Monte Perdido glacier and understand its recent evolution (López-Moreno *et al.*, 2019). By analysing the TLS data acquired over this period, we were able to track yearly changes in the glacier's surface elevation, thickness, and extent, providing crucial information about its dynamic behaviour.

The high-resolution topography of the glacier's surrounding area was obtained from the Centro Nacional de Información Geográfica (CNIG) (CNIG, 2023) (Fig. 2). Specifically, we utilised the Digital Elevation Model (DEM) with a 5 m grid resolution. This data allowed us to accurately represent the terrain and its influence on the glacier's behaviour. The glacier outlines were derived from the 2011 TLS (first year with observations), combining this information with topographical variables (Revuelto *et al.*, 2022). Additionally, GPR measurements were obtained in 2016 to capture the ice thickness of the Monte Perdido glacier along several observation transects with an uncertainty of 5 m (López-Moreno *et al.*, 2019).

We specifically focused on analysing the lower Monte Perdido glacier due to the higher availability of TLS and GPR (ground-penetrating radar) data.

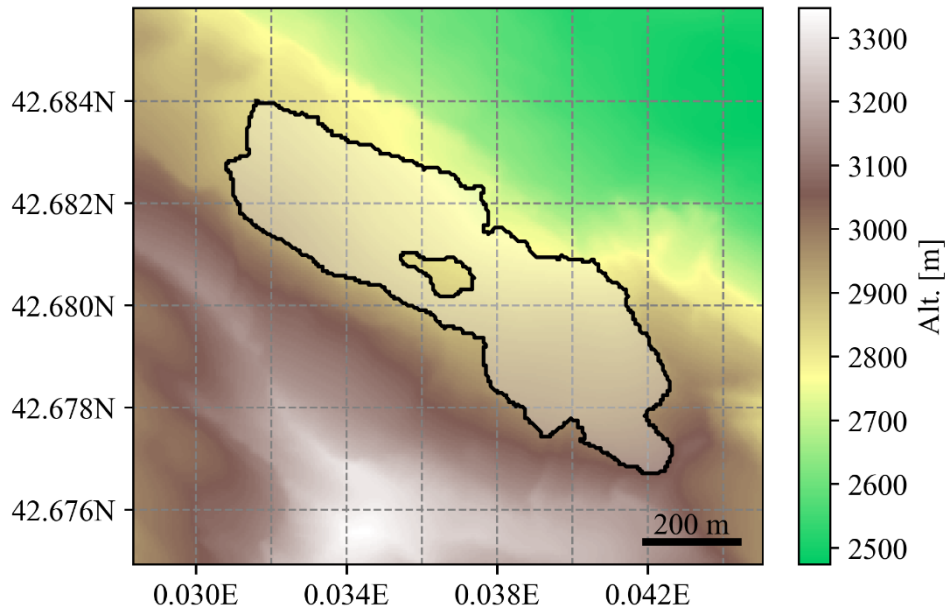


Figure 2: Outlines and DEM of glacier's surrounding area in 2011 (WGS84 coordinate system).

3.3. Climate data

We used long-term (1982-2022) monthly mean temperature and precipitation data obtained from a weather station located at the Góriz refuge (42.66335°N, 0.01501°E). This meteorological data, managed by the Spanish Meteorological Service (AEMET), was collected approximately 2.5 km from the glacier and at an elevation of 2195 m a.s.l. To adapt the data to the glacier region, we applied a lapse rate of 6.5 °C/km and a precipitation correction factor, which will be further explained in detail.

To ensure a continuous climate dataset, we addressed missing data from the weather station by utilising ERA5 reanalysis data (Hersbach *et al.*, 2023). Prior to filling the gaps, we evaluated the Góriz and ERA5 data during overlapping periods and applied the appropriate multiplication factor to precipitation and temperature. This approach was necessary to maintain data continuity for the OGGM. Furthermore, we have also used the GSWP3- W5E5 data set (Lange and Büchner, 2020), which is the default OGGM climate data. GSWP3-W5E5 dataset is a merge between the GSWP3 (Global Soil Wetness Projected phase 3) dataset (Dirmeyer *et al.*, 2006; Kim *et al.*, 2017) and the W5E5 (bias-adjusted ERA5 reanalysis) dataset (Lange, 2019; Cucchi *et al.*, 2020) at 0.5°x 0.5° spatial resolution.

For future projections, we selected a list of 10 global climate models from the Coupled Model Intercomparison Project Phase 5 (CMIP5) ensemble (Taylor *et al.*, 2012) (Table 1). By considering multiple GCMs, we aimed to capture a range of potential future climate scenarios and assess their impact on the glacier.

For CMIP5, four Representative Concentration Pathways (RCPs) have been formulated that provide insights into the expected levels of radiative forcing in the year 2100 when compared to preindustrial conditions (Taylor *et al.*, 2012). These pathways serve as estimations for the impact of greenhouse gas concentrations on the Earth's energy balance. Radiative forcing represents the net change in the energy balance of the Earth system, determined at the top of the atmosphere or the tropopause, due to natural or human-induced perturbations (Myhre *et al.*, 2013). For our analysis, we focused on the RCP2.6 and RCP8.5 scenarios, as they represent the two extremes within the RCP framework. RCP8.5 stands as the “high” scenario, projecting a continuous rise in radiative forcing throughout the twenty-first century until it reaches approximately 8.5 W/m² by the end of the century. Conversely, the RCP2.6 scenario assumes strong mitigation efforts with a radiative forcing of 2.6 W/m² by 2100 (Taylor *et al.*, 2012).

Table 1. CMIP5 models used in this study.

Model name	Resolution	Originating Group(s)	References
CCSM4	0.9°×1.2°	NCAR	Gent <i>et al.</i> , 2011
CNRM-CM5	1.4°×1.4°	CNRM-CERFACS	Voltaire <i>et al.</i> , 2013
CSIRO-Mk3-6-0	1.8°×1.8°	CSIRO-QCCCE	Rotstayn <i>et al.</i> , 2009
CanESM2	2.8°×2.8°	CCCMA	Arora <i>et al.</i> , 2011
GFDL-CM3	2.5°×2.0°	NOAA, GFDL	Donner <i>et al.</i> , 2011
GFDL-ESM2G	2.5°×2.0°	NOAA, GFDL	Dunne <i>et al.</i> , 2012
GISS-E2-R	2.5°×2.0°	NASA, GISS	Miller <i>et al.</i> , 2014
IPSL-CM5A-LR	3.7°×1.9°	IPSL	Hourdin <i>et al.</i> , 2006
MPI-ESM-LR	1.8°×1.8°	MPI-M	Zanchettin <i>et al.</i> , 2013
NorESM1-M	1.8°×2.5°	NCC	Bentsen <i>et al.</i> , 2013

3.4. Model calibration

To determine the volume evolution of our glacier, it is important to know how melt in a given period relates to the climate in the same period. This relationship is established by analysing a period in which we have available both climate data and thickness change, i.e., from 2011 to 2022. Once this calibration is done, we can predict glacier evolution applying future climate forcing to our glacier, assuming that the glacier response to climate forcing remains constant in the future.

For this calibration process, several steps using OGGM were involved. Firstly, we set up the geographical input data for the glacier, such as outlines and local topography. Then the climate data was processed from a user-defined climate file, and later the glacier flowlines were determined (Maussion *et al.*, 2019). Afterwards, we proceeded with the mass balance calibration process. For this, we employed OGGM's standard mass-balance (MB) model, which utilises a temperature index approach (Maussion *et al.*, 2019; Vlug, 2021). The basic assumption of these models is that the melt is proportional to the positive temperature in a certain period of time (Braithwaite and Zhang, 2000; Hock, 2003). This calibration determines specific glacier simulation parameters: the temperature bias, the precipitation factor and the degree-day factor (Maussion *et al.*, 2019; Schuster *et al.*, 2023).

The monthly temperature index model can be calibrated on any mass balance product. The default is the geodetic MB data from Hugonnet *et al.*, 2021, which consists of comparing the glacier surface, obtained from satellite elevation datasets, over two dates (Belart, 2018). This global geodetic glacier dataset provides a mean specific glacier MB estimate between 2000 and 2019 for almost every glacier on Earth (more than 200,000) (Schuster *et al.*, 2023). However, these geodetic estimates do not capture interannual variations and its spatial resolution is moderate when compared to TLS data. Alternatively, in situ mass balance measurements can be employed to capture the year-to-year changes.

The monthly mass balance B_i at elevation z is computed as follows:

$$B_i(z) = P_f P_i^{Solid}(z) - d_f \max(T_i(z) - T_{Melt}, 0) \quad (1)$$

Where monthly solid precipitation P_i^{Solid} is multiplied by the precipitation correction factor P_f . As there is no precipitation lapse rate in the model, P_f can be seen as a global correction factor for orographic precipitation, avalanches, and wind-blown snow (Vlug, 2021). The precipitation is assumed as liquid above 2°C, solid below 0°C, and the fraction of solid precipitation is linearly interpolated between these two boundary values. T_i is the monthly mean air temperature at 2 m and T_{Melt} is the monthly mean air temperature above which ice melt is assumed to occur (-1°C per default according to OGGM standard due to ice pressure). The temperature lapse rate is set by default to 6.5 °C/km. The parameter d_f is the degree-day factor indicating the temperature sensitivity of the glacier (van der Laan *et al.*, 2022; Schuster *et al.*, 2023).

We conducted three simulations (each with a specific calibration of three parameters: precipitation factor, temperature bias, and degree-day factor) to analyse the behaviour of glaciers under different configurations (Fig. 3, Table 2):

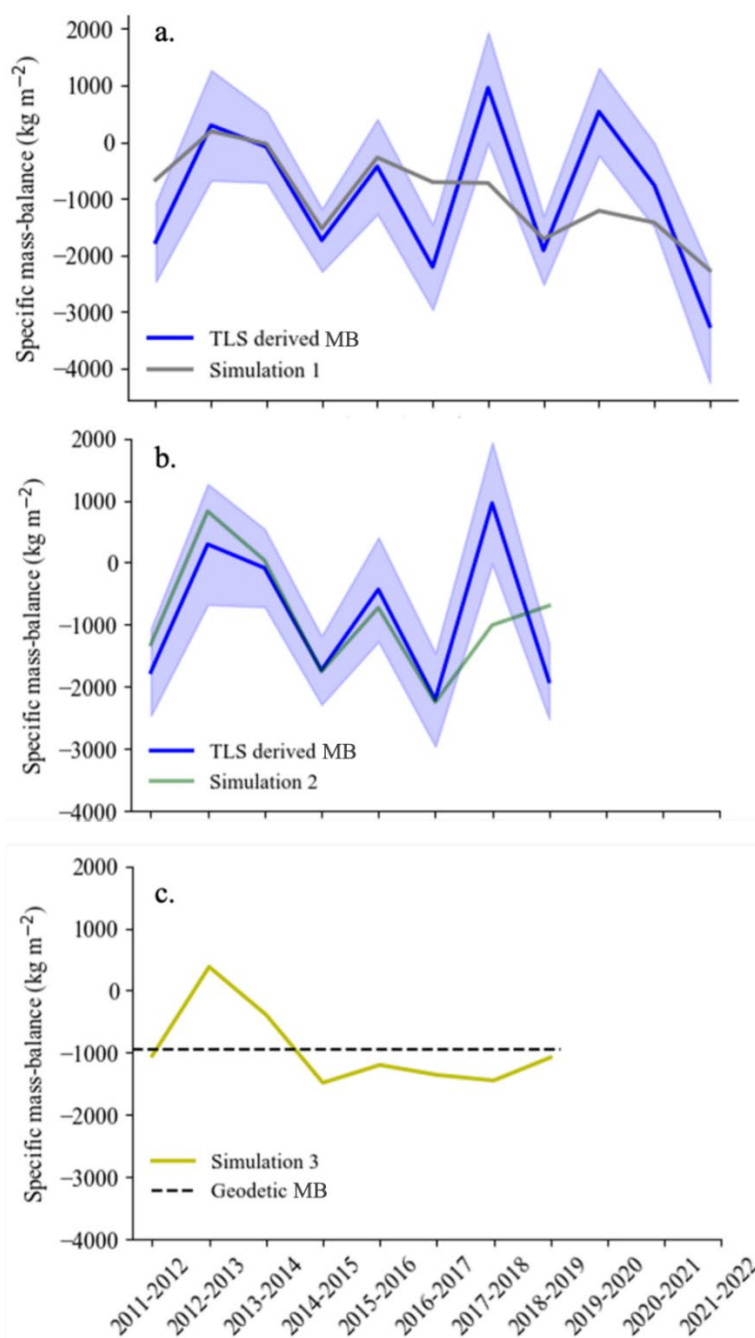


Figure 3: Comparison of TLS-derived mass balance (and its standard deviation (SD) and (a) modelled mass balance with in situ MB calibration and Góriz weather station climate data, (b) modelled mass balance with in situ MB calibration and GSWP3-W5E5 climate data, and (c) modelled mass balance with geodetic MB calibration.

Table 2. Data sources used for mass balance calibration and climate data in different simulations

	Data used for MB calibration	Climate data
Simulation 1	TLS	Góriz weather station
Simulation 2	TLS	GSWP3-W5E5
Simulation 3	Geodetic MB	GSWP3-W5E5

- Simulation 1: This simulation involved calibrating the mass balance using in situ data obtained from TLS for the years 2011 to 2022. The precipitation factor was estimated by comparing the total water equivalent of snow during the accumulation period (from October to April) at the glacier location (López-Moreno *et al.*, 2019) with the precipitation data recorded at the Góriz weather station for the same period. Analysis of specific years (2013-14, 2014-15, and 2016-17, which are the only periods with glacier surface observations during the accumulation period) revealed a maximum mean snow accumulation in late April of 3.25 m, with an average snow density of 454 kg/m³ (López-Moreno *et al.*, 2019). This indicated a total water equivalent of 1475.5 mm for the accumulation period. Considering that the mean precipitation observed at the Góriz weather station during the same period was 1089.6 mm, a precipitation factor of 1.3 was estimated and used for the mass balance calibration. Then, the model adjusted the degree-day factor and the temperature bias to minimise the difference between the model outputs and observed data, ensuring a better fit between the simulated and the actual mass balance.
- Simulation 2: As in the first simulation, this one involved mass balance calibration using TLS data. However, instead of using weather station climate data, we used the default climate data (GSWP3-W5E5) provided by the OGGM framework. The three parameters (precipitation factor, temperature bias, and degree-day factor) were adjusted accordingly.
- Simulation 3: In this simulation, the mass balance was calibrated with the default average geodetic observations from January 2000 to January 2019 of Hugonnet *et al.*, 2021, and the default climate data (GSWP3-W5E5) provided by OGGM.

All the calibration alternatives have at least the three free parameters mentioned above (Schuster *et al.*, 2023). Without these parameters, the observed glacier MB often cannot be reproduced by the model.

Once the mass balance calibration is performed, a standard geometry evolution model, which is a depth-integrated flowline model, is responsible to compute the change in glacier geometry. Before running this simulation, stable glacier conditions are required at the beginning of the study period. To ensure this, we performed a spin-up process, where the geometry and evolution of the glaciers were initialised from a given year. We selected a fixed geometry spin-up year of 2000, approximately 10 years before the date of the outline (2011). This year (2011) represents the point at which the glacier is expected to reach equilibrium (Maussion *et al.*, 2019).

Using the flowline model, an estimate of the ice flux along each glacier grid point cross-section is computed by making assumptions about the shape of the cross-section (parabolic, rectangular or trapezoid) and relying on mass-conservation consideration (Maussion *et al.*, 2019). Using the physics of ice flow and the shallow ice approximation, the model then computes the thickness of the glacier along the flowlines and the total volume of the glacier.

After performing the historical climate run, we used the ten GCMs described in Table 1 to project future volume of the Monte Perdido glacier. We employed an ensemble of GCMs to represent the temperature and precipitation variability in climate projections. To downscale global climate data to a regional level, we obtained precipitation and temperature data for each GCM from the OGGM server hosted by the University of Bremen and we applied the precipitation and temperature biases, to the baseline local climatology, which was defined using the Góriz weather station climate dataset. The model then uses the interpolated climate data for each GCM to calculate glacier mass balance.

Using this climate data, we ran the simulation for each GCM and scenario from 2020 to 2100. To initiate this task, we inputted the GCM climate data and utilised the spun up geometry and mass balance conditions from the historical run as initial conditions within the model.

Finally, we compiled the 20 simulations generated from the ensemble of GCMs and merged them into two datasets, one for each RCP scenario. This allowed us to calculate the median values and plot the evolution of glacier volume (Fig. 7).

4. Results and discussion

4.1. Evaluation of climate data

We first evaluate the GSWP3-W5E5 dataset from the OGGM repository against the data measured at the Góriz weather stations.

Figure 4a represents the historical annual temperature data measured at the Góriz weather station, along with the GSWP3-W5E5 dataset. The data reveals long-term temperature variations in the region, and a notable temperature rise on both datasets. The 30-year rolling average highlights this increase smoothing out short-term variations. The slope of $0.04^{\circ}\text{C}/\text{year}$ and the $p\text{-value} < 0.05$ on both datasets, confirm a statistically significant positive trend in temperature.

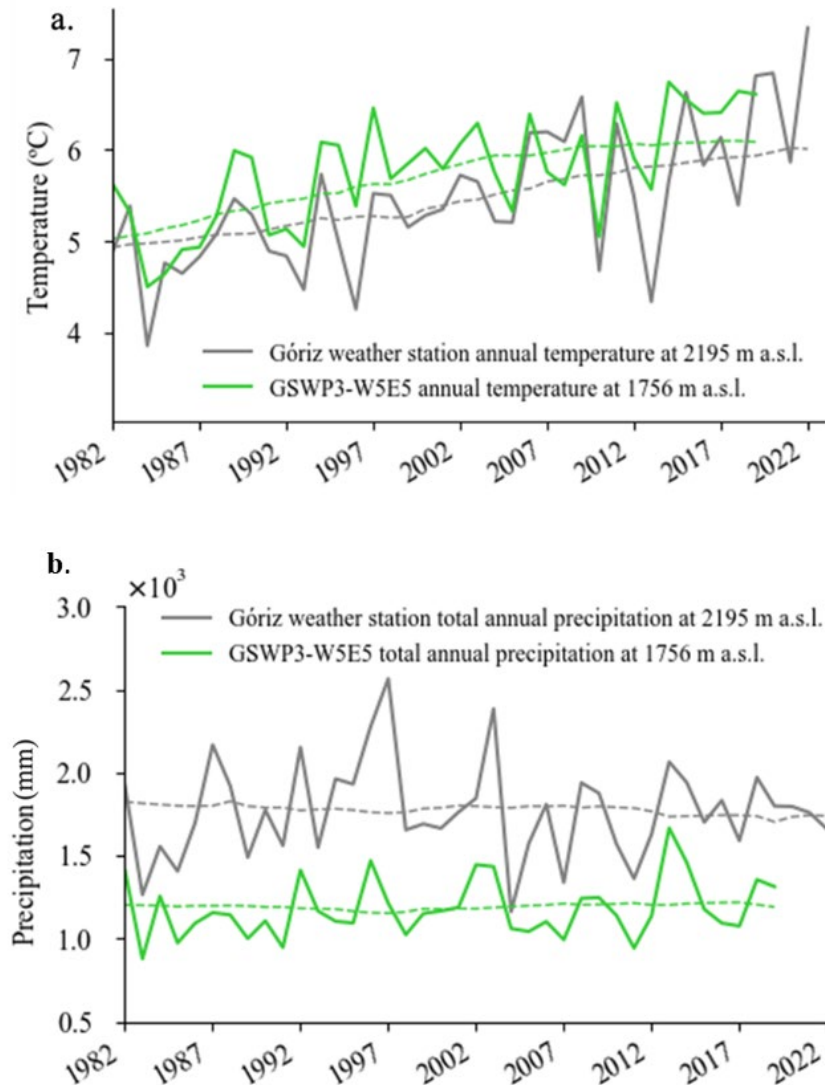


Figure 4: (a) Annual mean temperature and (b) total annual precipitation obtained from Góriz weather station (grey) and GSWP3-W5E5 dataset (green). The 30-year rolling average is depicted in dashed lines.

In addition, Figure 4b shows the historical total annual precipitation data obtained from the weather station and the GSWP3-W5E5 dataset. The data provides the interannual variability of precipitation over time. Unlike the temperature, there is no significant change in precipitation over time (p -value > 0.05). Furthermore, we observed a mean temperature difference of 0.4°C between the Góriz weather station, situated at 2195 m a.s.l., and the GSWP3-W5E5 dataset, located at 1756 m a.s.l. Additionally, the Góriz weather station records a greater total annual precipitation compared to the GSWP3-W5E5 dataset, with a difference of 590 mm.

4.2. Comparison of modelled and TLS-derived volume differences

The comparison of TLS volume evolution (surface decrease multiplied by glacier extent) and modelled volume evolution provides insights into the accuracy of the model in replicating the observed glacier volume changes (Fig. 5). The root mean square error (RMSE), correlation coefficient, and p -value were calculated to evaluate the model performance (Table 3).

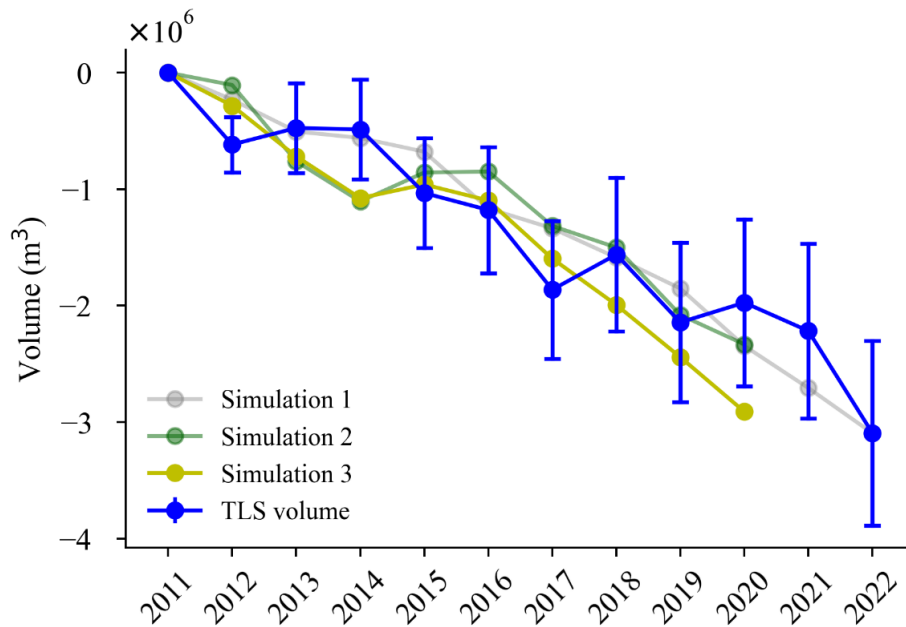


Figure 5: Monte Perdido glacier volume (and SD) since 2011 derived from TLS data compared with the three simulations.

Table 3. Comparison of TLS-Derived Volume with the three simulations from 2011 to 2020

	Corr.	p-value	RMSE (m ³)
Simulation 1	0.93	<0.01	279435.16
Simulation 2	0.92	<0.01	280778.70
Simulation 3	0.91	<0.01	418856.88

The results indicate that both simulations with in situ mass balance calibration, namely simulation 1 and 2, exhibit a higher correlation with the TLS-derived volume compared to simulation 3. This suggests that the calibration process with TLS data improves the agreement between the model and the observed data. Furthermore, simulation 1 with Góriz climate data shows slightly improved performance compared to the one with GSWP3- W5E5 climate data, as evidenced by a lower RMSE value and higher correlation coefficient (Table 3).

The incorporation of TLS data into the calibration process helps to account for the interannual variation of the glacier mass balance. This, in turn, enhances the accuracy of the model's predictions. Furthermore, Góriz climate data might provide a better representation of the local climate conditions and their influence on the glacier, resulting in a more accurate estimation of mass balance parameters.

It is important to note that simulation 3, despite exhibiting a slightly lower correlation and higher RMSE, still demonstrates a reasonable agreement with the TLS derived volume. This suggests that the calibration process, even with GSWP3-W5E5 climate data and geodetic mass balance calibration, can provide valuable insights into the glacier's behaviour. However, the differences in performance between simulation 3 and the other simulations highlight the importance of selecting appropriate climate data and calibration methods to improve the accuracy of glacier volume projections.

4.3. Comparison of modelled and GPR thickness

The GPR measurements, taken in 2016, offer a direct assessment of the glacier's ice thickness at specific locations on the Monte Perdido glacier (López-Moreno *et al.*, 2019). The comparison of modelled and GPR thickness provides additional insights into the accuracy of the model's representation of the spatial distribution of ice (Fig. 6).

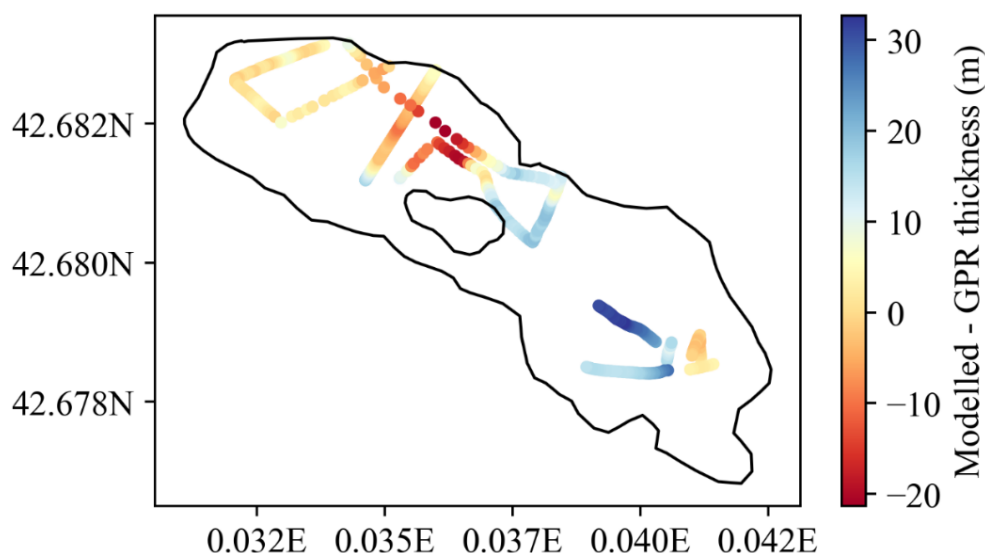


Figure 6: Difference between the modelled ice thickness and the GPR measurements taken in 2016 at specific locations of Monte Perdido glacier. WGS84 coordinate system.

It has to be noted that the GPR measurements were influenced by the presence of water, causing a very low signal to noise ratio leading to ± 5 m of uncertainty in estimations of ice thickness, which should be taken into account when interpreting the results.

The mean difference between the modelled and GPR thickness is 6.4 m, with a maximum difference of 32.7 m, indicating a certain level of variability and uncertainty in the model's ability to capture the ice thickness distribution. Furthermore, the average discrepancy between the two datasets is provided by the RMSE of 8.7 m. While there is some level of agreement between the model and the GPR data, there are still considerable differences between them.

However, it is important to note that GPR measurements provide localised information and may not fully represent the entire glacier's ice thickness distribution. Additionally, accurately modelling ice thickness is challenging without precise knowledge of the topography below the glacier.

Moreover, the weather station used for collecting meteorological data for the Monte Perdido glacier is situated about 2.5 km away from the glacier and on the south face, while the glacier itself is on the north face. This spatial difference introduces uncertainty in representing local climate conditions, despite applying temperature and precipitation correction factors. The use of a fixed lapse rate of 6.5°C/km to adjust weather station data to the glacier region simplifies temperature variations with elevation. Additionally, the estimation of the precipitation factor based on comparing data from the glacier location and a weather station may overlook variations in snowfall patterns, snow density, or liquid precipitation during the accumulation period.

4.4. Future volume projections

Across both RCP scenarios, the projected total ice volume for the Monte Perdido glacier shows a consistent decrease from 2020 to 2100. Figure 7 shows a faster decline in volume between 2020 and 2060, followed by a deceleration in the rate of decrease.

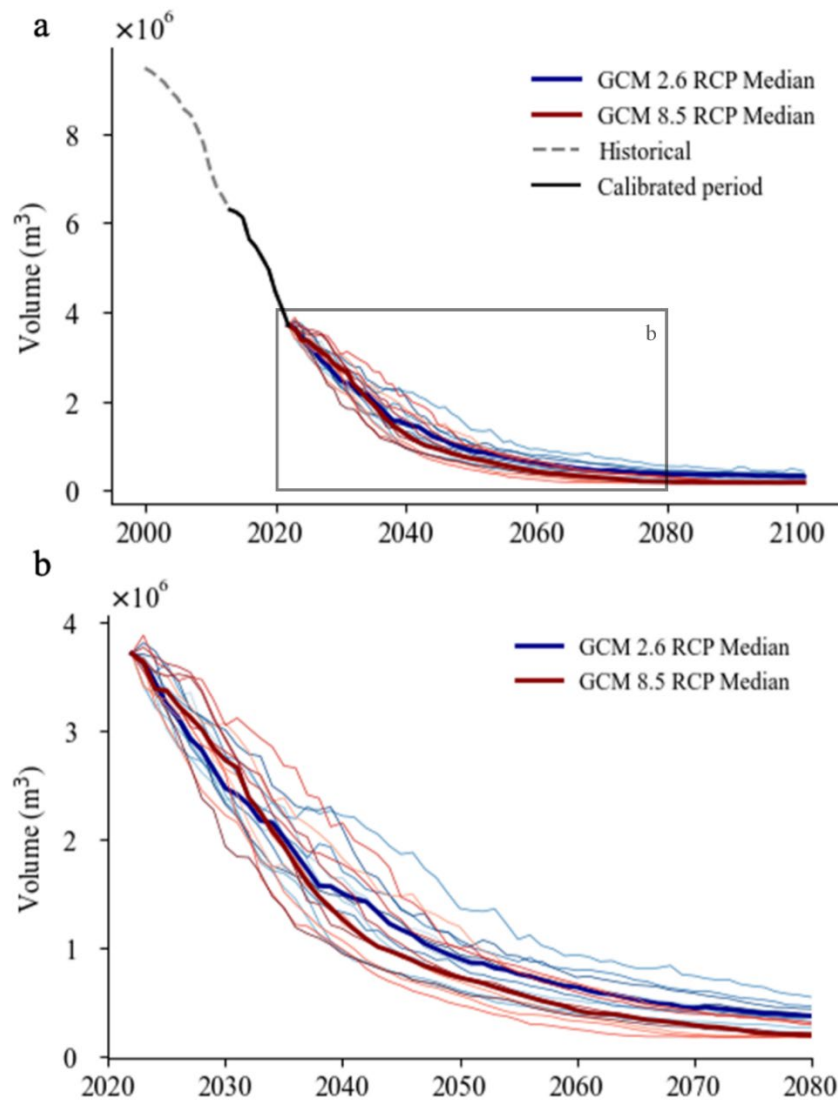


Figure 7: Multi-GCM ice volume for RCP2.6 and RCP8.5 scenarios from 2020 to 2100 with the historical simulation from 2000 to 2020 in a dashed line and the calibrated period in a solid black line. Volumes for each GCM run of RCP2.6 are plotted in blue and for RCP8.5 in red, with multi-GCM medians represented in thicker lines. Plot (a) displays the full projection, while (b) zooms the 2020 - 2080 period.

The total median volume exhibits minimal variation between the RCP scenarios. For the RCP8.5 scenario, the ice volume experiences a significant decrease of 95.2% by the year 2100, 88.6% by 2060, and 66.0% by 2040. Similarly, under the RCP2.6 scenario, there is a decrease of 91.6% by 2100, 82.8% by 2060, and 59.6% by 2040.

The observed decreasing trend in the volume of the Monte Perdido glacier is not unexpected; many studies have documented similar decreases in glacier volume worldwide (Ma *et al.*, 2010; Zekollari *et al.*, 2019; Khadka *et al.*, 2020), including in the Pyrenees (Chueca Cía *et al.*, 2005; López-Moreno *et al.*, 2016; Campos *et al.*, 2021; Vidaller *et al.*, 2021). Given that Monte Perdido is one of the largest glaciers of the Pyrenees, situated at higher altitudes and facing north, it suggests that other glaciers might experience even more pronounced losses.

5. Conclusions

We employed the Open Global Glacier Model to simulate and analyse the Monte Perdido glacier recent and future evolution. We utilised the OGGM to estimate the total ice volume of the glacier and simulate its evolution in response to different climate forcings.

The calibration process of the OGGM involved three simulations: one using in situ mass balance calibration and weather station climate data, another with in situ mass balance calibration using default climate data, and a third with uncalibrated mass balance and default climate data. Through these simulations, we evaluated the performance of the model when replicating the observed volume changes of the glacier. The simulations with in situ mass balance calibration exhibited a higher correlation with TLS-derived volume compared to the default MB geodetic calibration, indicating the importance of exploiting in-situ observations on the calibration to improve model accuracy.

Furthermore, we projected the future volume of the Monte Perdido glacier using an ensemble of ten GCMs under the RCP2.6 and RCP8.5 scenarios. The results showed a consistent decrease in total ice volume from 2020 to 2100, with a faster decline between 2020 and 2060 followed by a deceleration in the rate of decrease. The projected volume reductions were substantial, ranging from 91.6% to 95.2% by the year 2100, depending on the scenario. These findings align with the global trend of glacier volume decrease and are consistent with previous studies in the Pyrenees region.

In addition, as we look ahead, it's worth considering future directions that could further enhance our understanding of glacier behaviour and its interaction with climate. While our study primarily focused on the Monte Perdido glacier's response to climate forcing, we acknowledge the need for future investigations into the potential consequences of climate change on avalanche triggering and its subsequent impact on glacier evolution. Moreover, new approaches like ODINN.jl (Bolíbar *et al.*, 2023) and MuSA (Alonso-González *et al.*, 2022) demonstrate promising paths to enhance glacier modelling by incorporating advanced data assimilation techniques.

Acknowledgements

The authors are grateful for the OGGM community for developing and maintaining the OGGM model, AEMET, ISIMIP and the World Climate Research Programme's Working Group on Coupled Modelling for providing the necessary climate data and CNIG for granting access to their geospatial data. J. Revuelto is supported by a "Ramón y Cajal" postdoctoral fellow of the Spanish Ministry of Science, Innovation and Universities (RYC2021-033859-I). This work was partly supported by the project "MeltingIce: La desaparición de los últimos glaciares Pirenaicos" of the "Convocatoria 2023 de BECAS LEONARDO a Investigadores y Creadores Culturales Fundación BBVA".

References

- Alonso-González, E., Aalstad, K., Baba, M.W., Revuelto, J., López-Moreno, J.I., Fiddes, J., Essery, R., Gascoin, S., 2022. The Multiple Snow Data Assimilation System (MuSA v1.0). *Geoscientific Model Development* 15, 9127–9155. <https://doi.org/10.5194/gmd-15-9127-2022>
- Arora, V.K., Scinocca, J.F., Boer, G.J., Christian, J.R., Denman, K.L., Flato, G.M., Khari, V. V., Lee, W.G., Merryfield, W.J., 2011. Carbon emission limits required to satisfy future representative concentration pathways of greenhouse gases. *Geophysical Research Letters* 38 (5). <https://doi.org/10.1029/2010GL046270>
- Belart, J. M. C., 2018. *Mass balance of Icelandic glaciers in variable climate*. (Ph.D. thesis). University of Iceland; University of Toulouse III, Paul Sabatier.
- Beniston, M., 2003. Climatic Change in Mountain Regions: A Review of Possible Impacts. *Climatic Change* 59, 5–31. <https://doi.org/10.1023/A:1024458411589>
- Bentsen, M., Bethke, I., Debernard, J.B., Iversen, T., Kirkevåg, A., Seland, Ø., Drange, H., Roelandt, C., Seierstad, I.A., Hoose, C., Kristjánsson, J.E., 2013. The Norwegian Earth System Model, NorESM1-M – Part 1: Description and basic evaluation of the physical climate. *Geoscientific Model Development* 6 (3), 687–720. <https://doi.org/10.5194/gmd-6-687-2013>
- Bolibar, J., Sapienza, F., Maussion, F., Lguensat, R., Wouters, B., Pérez, F., 2023. Universal Differential Equations for glacier ice flow modelling. *Geoscientific Model Development Discussions* 16 (22), 6671–6687. <https://doi.org/10.5194/gmd-16-6671-2023>
- Braithwaite, R.J., Zhang, Y., 2000. Sensitivity of mass balance of five Swiss glaciers to temperature changes assessed by tuning a degree-day model. *Journal of Glaciology* 46, 7–14. <https://doi.org/10.3189/172756500781833511>
- Campos, N., Alcalá-Reygosa, J., Watson, S.C., Koukoulos, I., Quesada-Román, A., Grima, N., 2021. Modeling the retreat of the Aneto Glacier (Spanish Pyrenees) since the Little Ice Age, and its accelerated shrinkage over recent decades. *The Holocene* 31, 1315–1326. <https://doi.org/10.1177/09596836211011678>
- Centro Nacional de Información Geográfica (CNIG), 2023. Organismo Autónomo Centro Nacional de Información Geográfica (CNIG). <http://www.cnig.es>
- Chueca Cía, J., Julián Andrés, A., Saz Sánchez, M.A., Creus Novau, J., López Moreno, J.I., 2005. Responses to climatic changes since the Little Ice Age on Maladeta Glacier (Central Pyrenees). *Geomorphology* 68, 167–182. <https://doi.org/10.1016/j.geomorph.2004.11.012>
- Cucchi, M., Weedon, G.P., Amici, A., Bellouin, N., Lange, S., Müller Schmied, H., Hersbach, H., Buontempo, C., 2020. WFDE5: bias-adjusted ERA5 reanalysis data for impact studies. *Earth System Science Data* 12, 2097–2120. <https://doi.org/10.5194/essd-12-2097-2020>
- Dirmeyer, P.A., Gao, X., Zhao, M., Guo, Z., Oki, T., Hanasaki, N., 2006. GSWP-2: Multimodel analysis and implications for our perception of the land surface. *Bulletin of the American Meteorological Society* 87, 1381–1398. American Meteorological Society. <https://doi.org/10.1175/BAMS-87-10-1381>
- Donner, L.J., Wyman, B.L., Hemler, R.S., Horowitz, L.W., Ming, Y., Zhao, M., Golaz, J.-C., Ginoux, P., Lin, S.-J., Schwarzkopf, M.D., Austin, J., Alaka, G., Cooke, W.F., Delworth, T.L., Freidenreich, S.M., Gordon, C.T., Griffies, S.M., Held, I.M., Hurlin, W.J., Klein, S.A., Knutson, T.R., Langenhorst, A.R., Lee, H.-C., Lin, Y., Magi, B.I., Malyshev, S.L., Milly, P.C.D., Naik, V., Nath, M.J., Pincus, R., Ploshay, J.J., Ramaswamy, V., Seman, C.J., Shevliakova, E., Sirutis, J.J., Stern, W.F., Stouffer, R.J., Wilson, R.J., Winton, M., Wittenberg, A.T., Zeng, F., 2011. The Dynamical Core, Physical Parameterizations, and Basic Simulation Characteristics of the Atmospheric Component AM3 of the GFDL Global Coupled Model CM3. *Journal of Climate* 24, 3484–3519. <https://doi.org/10.1175/2011JCLI3955.1>
- Dunne, J.P., John, J.G., Adcroft, A.J., Griffies, S.M., Hallberg, R.W., Shevliakova, E., Stouffer, R.J., Cooke, W., Dunne, K.A., Harrison, M.J., Krasting, J.P., Malyshev, S.L., Milly, P.C.D., Phillipps, P.J., Sentman, L.T., Samuels, B.L., Spelman, M.J., Winton, M., Wittenberg, A.T., Zadeh, N., 2012. GFDL's ESM2 Global Coupled Climate–Carbon Earth System Models. Part I: Physical Formulation and Baseline Simulation Characteristics. *Journal of Climate* 25, 6646–6665. <https://doi.org/10.1175/JCLI-D-11-00560.1>
- Eis, J., 2020. *Reconstructing glacier evolution using a flowline model-Development of an initialization method*. University of Bremen.

- Farinotti, D., Huss, M., Bauder, A., Funk, M., Truffer, M., 2009. A method to estimate the ice volume and ice-thickness distribution of alpine glaciers. *Journal of Glaciology* 55, 422–430. <https://doi.org/10.3189/002214309788816759>
- García-López, E., Moreno, A., Bartolomé, M., Leunda, M., Sancho, C., Cid, C., 2021. Glacial Ice Age Shapes Microbiome Composition in a Receding Southern European Glacier. *Frontiers in Microbiology*, 12. <https://doi.org/10.3389/fmicb.2021.714537>
- Gent, P.R., Danabasoglu, G., Donner, L.J., Holland, M.M., Hunke, E.C., Jayne, S.R., Lawrence, D.M., Neale, R.B., Rasch, P.J., Vertenstein, M., Worley, P.H., Yang, Z.-L., Zhang, M., 2011. The Community Climate System Model Version 4. *Journal of Climate* 24, 4973–4991. <https://doi.org/10.1175/2011JCLI4083.1>
- Grunewald, K., Scheithauer, J., 2010. Europe’s southernmost glaciers: response and adaptation to climate change. *Journal of Glaciology* 56, 129–142. <https://doi.org/10.3189/002214310791190947>
- Hersbach, H., Bell, B., Berrisford, P., Biavati, G., Horányi, A., Muñoz Sabater, J., Nicolas, J., Peubey, C., Radu, R., Rozum, I., Schepers, D., Simmons, A., Soci, C., Dee, D., Thépaut, J.-N., 2023. ERA5 monthly averaged data on single levels from 1940 to present. <https://doi.org/10.24381/cds.fl7050d7>
- Hock, R., 2003. Temperature index melt modelling in mountain areas. *Journal of Hydrology* 282, 104–115. [https://doi.org/10.1016/S0022-1694\(03\)00257-9](https://doi.org/10.1016/S0022-1694(03)00257-9)
- Hourdin, F., Musat, I., Bony, S., Braconnot, P., Codron, F., Dufresne, J.-L., Fairhead, L., Filiberti, M.-A., Friedlingstein, P., Grandpeix, J.-Y., Krinner, G., LeVan, P., Li, Z.-X., Lott, F., 2006. The LMDZ4 general circulation model: climate performance and sensitivity to parametrized physics with emphasis on tropical convection. *Climate Dynamics* 27, 787–813. <https://doi.org/10.1007/s00382-006-0158-0>
- Hugonnet, R., McNabb, R., Berthier, E., Menounos, B., Nuth, C., Girod, L., Farinotti, D., Huss, M., Dussailant, I., Brun, F., Kääb, A., 2021. Accelerated global glacier mass loss in the early twenty-first century. *Nature* 592, 726–731. <https://doi.org/10.1038/s41586-021-03436-z>
- Huston, A., Siler, N., Roe, G.H., Pettit, E., Steiger, N.J., 2021. Understanding drivers of glacier-length variability over the last millennium. *The Cryosphere* 15, 1645–1662. <https://doi.org/10.5194/tc-15-1645-2021>
- Huybers, K., Roe, G.H., 2009. Spatial Patterns of Glaciers in Response to Spatial Patterns in Regional Climate. *Journal of Climate* 22, 4606–4620. <https://doi.org/10.1175/2009JCLI2857.1>
- IPCC, 2021. *Climate change 2021: the physical science basis*. Contribution of working group I to the sixth assessment report of the intergovernmental panel on climate change.
- Julián, A., Chueca, J., 2007. Pérdidas de extensión y volumen en los glaciares del macizo de Monte Perdido (Pirineo central español): 1981–1999. *Boletín Glaciológico Aragonés* 8, 31–60.
- Khadka, M., Kayastha, R.B., Kayastha, R., 2020. Future projection of cryospheric and hydrologic regimes in Koshi River basin, Central Himalaya, using coupled glacier dynamics and glacio-hydrological models. *Journal of Glaciology* 66, 831–845. <https://doi.org/10.1017/jog.2020.51>
- Kienholz, C., Rich, J.L., Arendt, A.A., Hock, R., 2014. A new method for deriving glacier centerlines applied to glaciers in Alaska and northwest Canada. *The Cryosphere* 8, 503–519. <https://doi.org/10.5194/tc-8-503-2014>
- Kim, H., Watanabe, S., Chang, E.C., Yoshimura, K., Hirabayashi, J., Famiglietti, J., Oki, T., 2017. *Global Soil Wetness Project Phase 3 Atmospheric Boundary Conditions (Experiment 1)* [Data set], Data Integration and Analysis System (DIAS).
- Lange, S., 2019. WFDE5 over land merged with ERA5 over the ocean (W5E5). V. 1.0. *GFZ Data Services*.
- Lange, S., Büchner, M., 2020. *ISIMIP2a atmospheric climate input data*. ISIMIP Repository. <https://data.isimip.org/10.48364/ISIMIP.886955>
- López-Moreno, J.I., Revuelto, J., Rico, I., Chueca-Cía, J., Julián, A., Serreta, A., Serrano, E., Vicente-Serrano, S.M., Azorin-Molina, C., Alonso-González, E., García-Ruiz, J.M., 2016. Thinning of the Monte Perdido Glacier in the Spanish Pyrenees since 1981. *The Cryosphere* 10, 681–694. <https://doi.org/10.5194/tc-10-681-2016>
- López-Moreno, J.I., Alonso-González, E., Monserrat, O., Río, L.M. Del, Otero, J., Lapazaran, J., Luzi, G., Dematteis, N., Serreta, A., Rico, I., Serrano-Cañadas, E., Bartolomé, M., Moreno, A., Buisan, S., Revuelto, J., 2019. Ground-based remote-sensing techniques for diagnosis of the current state and recent

- evolution of the Monte Perdido Glacier, Spanish Pyrenees. *Journal of Glaciology* 65, 85–100. <https://doi.org/10.1017/jog.2018.96>
- López-Moreno, J.I., García-Ruiz, J.M., Vicente-Serrano, S.M., Alonso-González, E., Revuelto-Benedí, J., Rico, I., Izagirre, E., Beguería-Portugués, S., 2020. Critical discussion of: “A farewell to glaciers: Ecosystem services loss in the Spanish Pyrenees”. *Journal of Environmental Management* 275, 111247. <https://doi.org/10.1016/j.jenvman.2020.111247>
- Ma, L., Tian, L., Pu, J., Wang, P., 2010. Recent area and ice volume change of Kangwure Glacier in the middle of Himalayas. *Chinese Science Bulletin* 55, 2088–2096. <https://doi.org/10.1007/s11434-010-3211-7>
- Maussion, F., Butenko, A., Champollion, N., Dusch, M., Eis, J., Fourteau, K., Gregor, P., Jarosch, A.H., Landmann, J., Oesterle, F., Recinos, B., Rothenpieler, T., Vlug, A., Wild, C.T., Marzeion, B., 2019. The Open Global Glacier Model (OGGM) v1.1. *Geoscientific Model Development* 2019, 909–931. <https://doi.org/10.5194/gmd-12-909-2019>
- Maussion, F., Rothenpieler, T., Dusch, M., Schmitt, P., Vlug, A., Schuster, L., Champollion, N., Li, F., Marzeion, B., Oberrauch, M., Eis, J., Landmann, J., Jarosch, A., Fischer, A., Iuzpaz, Hanus, S., Rounce, D., Castellani, M., Bartholomew, S.L., Minallah, S., bowenbelongstonature, Merrill, C., Otto, D., Loibl, D., Ultee, L., Thompson, S., anton-ub, Gregor, P., zhaohongyu, 2023. OGGM/oggm: v1.6.0. Zenodo. <https://doi.org/10.5281/zenodo.7718476>
- Miller, R.L., Schmidt, G.A., Nazarenko, L.S., Tausnev, N., Bauer, S.E., DelGenio, A.D., Kelley, M., Lo, K.K., Ruedy, R., Shindell, D.T., Aleinov, I., Bauer, M., Bleck, R., Canuto, V., Chen, Y., Cheng, Y., Clune, T.L., Faluvegi, G., Hansen, J.E., Healy, R.J., Kiang, N.Y., Koch, D., Lacis, A.A., LeGrande, A.N., Lerner, J., Menon, S., Oinas, V., García-Pando, C.P., Perlwitz, J.P., Puma, M.J., Rind, D., Romanou, A., Russell, G.L., Sato, M., Sun, S., Tsigaridis, K., Unger, N., Voulgarakis, A., Yao, M.-S., Zhang, J., 2014. CMIP5 historical simulations (1850–2012) with GISS ModelE2. *Journal of Advances in Modeling Earth Systems* 6, 441–478. <https://doi.org/10.1002/2013MS000266>
- Moreno, A., Bartolomé, M., López-Moreno, J.I., Pey, J., Corella, J.P., García-Orellana, J., Sancho, C., Leunda, M., Gil-Romera, G., González-Sampériz, P., Pérez-Mejías, C., Navarro, F., Otero-García, J., Lapazarán, J., Alonso-González, E., Cid, C., López-Martínez, J., Oliva-Urcia, B., Faria, S.H., Sierra, M.J., Millán, R., Querol, X., Alastuey, A., García-Ruiz, J.M., 2021. The case of a southern European glacier which survived Roman and medieval warm periods but is disappearing under recent warming. *The Cryosphere* 15, 1157–1172. <https://doi.org/10.5194/tc-15-1157-2021>
- Myhre, G., Shindell, D., Bréon, F.-M., Collins, W., Fuglestedt, J., Huang, J., Koch, D., Lamarque, J.-F., Lee, D., Mendoza, B., Nakajima, T., Robock, A., Stephens, G., Takemura, T., Zhang, H., 2013. *Anthropogenic and natural radiative forcing*. P. in: *Climate Change 2013: The Physical Science Basis. Contribution of Working Group I to the Fifth Assessment Report of the Intergovernmental Panel on Climate Change*. Cambridge University Press, 659–740 pp.
- Paterson, W.S.B., 2000. *Physics of glaciers*. P. in.: Butterworth-Heinemann.
- Revuelto, J., López-Moreno, J.I., Azorin-Molina, C., Zabalza, J., Arguedas, G., Vicente-Serrano, S.M., 2014. Mapping the annual evolution of snow depth in a small catchment in the Pyrenees using the long-range terrestrial laser scanning. *Journal of Maps* 10, 379–393. <https://doi.org/10.1080/17445647.2013.869268>
- Revuelto, J., Jiménez, J.G., Rojas-Heredia, F., Vidaller, I., Deschamps-Berger, C., Izagirre, E., Voordendag, A., López-Moreno, J.I., 2022. Geometric features of mountain glaciers from 3D point clouds to delimit their extent: insight from gradient boosting trees algorithms. Pp. C55A–01 in: *AGU Fall Meeting Abstracts*.
- Rico, I., Izagirre, E., Serrano, E., López-Moreno, J.I., 2017. Superficie glaciaria actual en los Pirineos: Una actualización para 2016. *Pirineos* 172, 29. <https://doi.org/10.3989/Pirineos.2017.172004>
- Rotstayn, L.D., Collier, M.A., Dix, M.R., Feng, Y., Gordon, H.B., O’Farrell, S.P., Smith, I.N., Syktus, J., 2009. Improved simulation of Australian climate and ENSO-related rainfall variability in a global climate model with an interactive aerosol treatment. *International Journal of Climatology* 30 (7), 1067–1088. <https://doi.org/10.1002/joc.1952>
- Schuster, L., Rounce, D.R., Maussion, F., 2023. Glacier projections sensitivity to temperature-index model choices and calibration strategies. *Annals of Glaciology*. <https://doi.org/10.1017/aog.2023.57>
- Serrano Cañadas, E., 2023. *Glaciares, cultura y patrimonio La huella cultural de los glaciares pirenaicos*. Universidad de Valladolid.

- Taylor, K.E., Stouffer, R.J., Meehl, G.A., 2012. An Overview of CMIP5 and the Experiment Design. *Bulletin of the American Meteorological Society* 93, 485–498. <https://doi.org/10.1175/BAMS-D-11-00094.1>
- Van der Laan, L.N., Cholibois, K., El Menuawy, A., Förster, K., 2022. A Scenario-Neutral Approach to Climate Change in Glacier Mass Balance Modelling. *Annals of Glaciology*. <https://doi.org/10.31223/X51H18>
- Van der Veen, C.J., 2013. *Fundamentals of Glacier Dynamics*. CRC Press.
- Vidaller, I., Revuelto, J., Izagirre, E., Rojas-Heredia, F., Alonso-González, E., Gascoïn, S., René, P., Berthier, E., Rico, I., Moreno, A., Serrano, E., Serreta, A., López-Moreno, J.I., 2021. Toward an Ice-Free Mountain Range: Demise of Pyrenean Glaciers During 2011–2020. *Geophysical Research Letters*, 48 (18). <https://doi.org/10.1029/2021GL094339>
- Vlug, A., 2021. *The influence of climate variability on the mass balance of Canadian Arctic land-terminating glaciers, in simulations of the last millennium*. Universität Bremen.
- Voldoire, A., Sanchez-Gomez, E., y Méliá, D.S., Decharme, B., Cassou, C., Sénési, S., Valeke, S., Beau, I., Alias, A., Chevallier, M., Déqué, M., Deshayes, J., Douville, H., Fernandez, E., Madec, G., Maisonnave, E., Moine, M.-P., Planton, S., Saint-Martin, D., Szopa, S., Tyteca, S., Alkama, R., Belamari, S., Braun, A., Coquart, L., Chauvin, F., 2013. The CNRM-CM5.1 global climate model: description and basic evaluation. *Climate Dynamics*, 40, 2091–2121. <https://doi.org/10.1007/s00382-011-1259-y>
- Zanchettin, D., Rubino, A., Matei, D., Bothe, O., Jungclauss, J.H., 2013. Multidecadal-to-centennial SST variability in the MPI-ESM simulation ensemble for the last millennium. *Climate Dynamics* 40, 1301–1318. <https://doi.org/10.1007/s00382-012-1361-9>
- Zekollari, H., Huss, M., Farinotti, D., 2019. Modelling the future evolution of glaciers in the European Alps under the EURO-CORDEX RCM ensemble. *The Cryosphere* 13, 1125–1146. <https://doi.org/10.5194/tc-13-1125-2019>